MECHANISM OF THE ^{7}Li$(d,t)^6$Li REACTION AT 25 MeV ENERGY OF DEUTERONS, VALUES OF SPECTROSCOPIC FACTORS AND ASYMPTOTIC NORMALIZATION COEFFICIENTS FOR THE $^7\text{Li} \to {}^6\text{Li} + n$ VERTEX

N. Burtebayev[a], J.T. Burtebayeva[a], A. Duisebayev[a]
Zh.K. Kerimkulov[a], M. Nassurlla[a], T. Zholdybayev[a]
S.V. Artemov[b], A.A. Karakhodzhayev[b], U.S. Salikhbayev[b]
S.B. Sakuta[c], S. Kliczewski[d], E. Piasecki[e], K. Rusek[e]
R. Siudak[d], A. Trzcińska[e], M. Wolińska-Cichocka[e], A. Amar[f]

[a]Institute of Nuclear Physics, Ibragimova 1, 050032 Almaty, Kazakhstan
[b]Institute of Nuclear Physics, settl. Ulugbek, 100214 Tashkent, Uzbekistan
[c]National Research Center "Kurchatov Institute"
Kurchatov Sq. 1, 123182 Moscow, Russia
[d]The Henryk Niewodniczański Institute of Nuclear Physics
Polish Academy of Sciences
Radzikowskiego 152, 31-342 Kraków, Poland
[e]Heavy Ion Laboratory of University of Warsaw
Pasteura 5A, 02-093 Warszawa, Poland
[f]Tanta University, Faculty of Science, Physics Department, Tanta, Egypt

(Received January 7, 2015; revised version received March 16, 2015)

Angular distributions of deuterons elastically and inelastically scattered on ^{7}Li nuclei with excitation of the 0.478 MeV ($J^\pi = 1/2^-$) level, and tritons from the ^{7}Li$(d,t)^6$Li reaction, corresponding to transitions to the ground ($J^\pi = 1^+$) and low-lying excited states ($J^\pi = 3^+$ and 0^+) of the ^{6}Li nucleus were measured at the 25 MeV energy. The experimental data were analyzed within the framework of the coupled reaction channels and a modified distorted-wave methods. The values of the spectroscopic factors and the asymptotic normalization coefficients for the $^7\text{Li} \to {}^6\text{Li} + n$ vertex were extracted.

DOI:10.5506/APhysPolB.46.1037
PACS numbers: 24.50.+g, 24.10.Eq, 25.45.Hi

1. Introduction

Study of the interaction of charged particles with lithium nuclei is of great interest. On the one hand, lithium is one of the most important elements of the fuel cycle in the promising projects of the fusion reactors using

deuterium–tritium plasma. Current technologies of thermonuclear synthesis require knowledge of the interaction cross sections of light nuclei ($Z \leq 4$) with high accuracy. The ^{7}Li$(d,t)^6$Li reaction with the production of tritium is of particular interest for applications [1]. Unfortunately, information about it is very limited, as we shall see below. Another aspect is related to the problem of lithium isotopes in the standard big bang nucleosynthesis: overestimation of ^{7}Li and underestimation of ^{6}Li abundances [2, 3]. In particular, all reactions which come to ^{6,7}Li formation or destroy should be inspected. Previously obtained values of the asymptotic normalization coefficient (ANC) for the $^7\text{Be} \to {}^6\text{Li} + p$ system would be useful to compare with the value of ANC for the mirror configuration $^7\text{Li} \to {}^6\text{Li} + n$, which can be obtained from the analysis of the experimental cross sections of the ^{7}Li$(d,t)^6$Li reaction with potentials describing the interaction of deuterons with ^{7}Li and t (^{3}He) with ^{6}Li nuclei. Such analysis is usually carried out in the framework of the optical model and distorted-wave Born approximation (DWBA). However, the applicability of these models to the lightest nuclei encounters serious difficulties. Firstly, the level density of compound systems is relatively low for light nuclei. The strong energy dependence of the cross sections, especially at low energies, may be observed due to insufficient averaging the resonant states in the interaction of the colliding nuclei. Secondly, the role of cluster effects is enhanced due to small number of particles. That is the reason why the standard optical model, and hence the conventional distorted-wave method does not have a rigorous substantiation and remains unsatisfactory for obtaining reliable spectroscopic information. Values of the spectroscopic factors (SF) extracted from the analysis of experimental differential cross sections using the DWBA are often contradictory.

The (d,t) reaction on the ^{7}Li nuclei were previously studied at 12 MeV [4, 5], 15 MeV [6, 7], 18 MeV [8], 20 MeV [9] and 28 MeV [10] energies. The measurements in the full angular range were done at $E_d = 12$ MeV [4] only. In other cases, they were performed in the forward hemisphere. The standard DWBA with zero and finite-range interaction, used in the calculation of the angular distributions in [4, 5], does not describe the experimental cross sections at large angles. The calculations at other energies (15, 20, 28 MeV) were only qualitative using the plane wave Born approximation (PWBA) with Butler formula for pick-up reactions [6, 9, 10]. The values of the spectroscopic factors were not extracted.

Progress in description of the (d,t) reaction using DWBA has been achieved by a combination of DWBA and dispersion relations [8]. If the reaction goes on the periphery of the nucleus, the modified DWBA should be used, where the differential cross section is parameterized by the vertex constant (or ANC which is the same up to a constant factor, see Subsection 3.2.). This method allows to select a purely peripheral reaction with the

dominance of a pole mechanism. The analysis of the experimental angular distributions of the (d,t) reactions on a number of light nuclei at energies of deuterons from 12 to 50 MeV has shown that these reactions are purely peripheral. However, in the case of ^{7}Li, the obtained value of the squared module of the vertex constant $|G|^2$ for $^7\text{Li} \to {}^6\text{Li} + n$ vertex depends on the energy and varies from 1.5 fm ($E_d = 12$ MeV) to 0.3 fm ($E_d = 28$ MeV) [8]. This is due (according to [8]) to the contribution of non-pole mechanisms.

Difficulties in describing the reaction $^7\text{Li}(d,t)$ with DWBA can be also due to neglecting the channel coupling as well as contribution of the exchange processes. Their role is still unexplored. The ^{7}Li nucleus is strongly deformed and has a quadrupole momentum $Q = 40.6$ mb. The reduced probability of electric quadrupole transition $3/2^-$ (ground state) $\to 1/2^-$ ($E_x = 0.478$ MeV) for ^{7}Li nucleus is equal to the value of $B(\text{E2}) = 8.3\ e^2\text{fm}^4$ [11]. Although ^{6}Li has a much lower value of the quadrupole momentum ($Q = 0.818$ mb), and then (from this point of view) is almost spherical, the reduced probability of electric quadrupole transition from the ground state ($J^\pi = 1^+$) to the first excited state ($J^\pi = 3^+$, $E_x = 2.186$ MeV) is equal to $B(\text{E2}) = 25.6\ e^2\text{fm}^4$ and is almost an order of magnitude greater than the probability of one-particle transition [11, 12]. Therefore, the effects of channel coupling of the elastic and inelastic scattering cannot be neglected. In addition, the ^{7}Li nucleus has a weakly bound structure $^7\text{Li} = \alpha + t$, and, in this case, the exchange mechanism with α-particle transfer $^7\text{Li}(d,\ ^6\text{Li})t$ can give a significant contribution to the cross section of the $^7\text{Li}(d,t)^6\text{Li}$ reaction.

The aims of this work are investigation of the $^7\text{Li}(d,t)^6\text{Li}$ reaction at the 25 MeV energy, analysis of the experimental data with taking into account the channel coupling and α-particles exchange mechanism, obtaining information about the spectroscopic factors and asymptotic normalization coefficients in the framework of the modified DWBA (MDWBA).

2. Experimental method and results

The experiment was performed using the deuteron beam with 25 MeV energy, extracted from the U-150 isochronous Cyclotron of Institute of Nuclear Physics (Almaty, Kazakhstan). Differential cross sections for elastic and inelastic scattering of deuterons and tritons from the reaction (d,t) on ^{7}Li nuclei were measured in the angular range from 8° to 169° (LAB), except of the range of angles 77°–107°, where it was impossible because of the design of the target device.

The metal lithium with 99% enrichment of ^{7}Li was used as a target. It was manufactured by thermal evaporation of lithium on a thin alundum (Al_2O_3) film ($\sim 30\ \mu\text{g/cm}^2$) in vacuum. After deposition, the target was

transferred to a scattering chamber without breaking the vacuum. The thicknesses of lithium layers, determined by the energy losses of α-particles from a radioactive source were 300–330 μg/cm^2. The design of the scattering chamber is described in detail in [13].

Deuterons and tritons were detected and identified using the ΔE–E-telescope of two silicon counters with thicknesses of 100 microns and 2 mm. The total energy resolution was 250–300 keV. It was determined mainly by energy spread of the beam and target thickness.

The typical deuterons and tritons spectra are shown in Fig. 1. In the deuteron spectra (Fig. 1, top), transitions to the states at excitation energies $E_x = 0.478$ MeV $(1/2^-)$ and 4.65 MeV $(7/2^-)$ in addition to the elastic peak were observed. Scattering of deuterons on carbon and oxygen impurities affects the accuracy of measurements of the cross sections for 4.65 MeV state only. Therefore, this state was excluded from further analysis. Sepa-

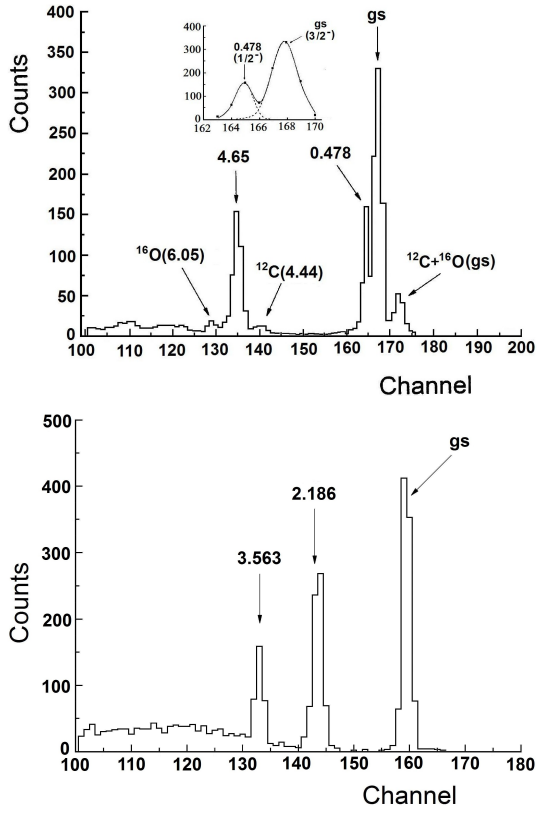

Fig. 1. Spectrum of deuterons scattered by ^{7}Li nuclei at $\theta_{\rm LAB} = 22°$ angle with a beam energy of 25 MeV (top) and spectrum of tritons at $\theta_{\rm LAB} = 8°$ angle from the ^{7}Li$(d,t)^6$Li reaction (bottom).

ration of partly overlapped peaks of the elastic and inelastic scattering with excitation of the $E_x = 0.478$ MeV state was made by decomposition of the overall structure into two peaks of Gaussian shape, as shown in the inset (Fig. 1, top).

Three intensive groups of tritons, corresponding to the ground (1^+) and excited states of ^{6}Li ($E_x = 2.186$ MeV (3^+) and 3.563 MeV (0^+, $T = 1$)) were observed in the spectrum of the ^{7}Li$(d,t)^6$Li reaction (Fig. 1, bottom). The contribution of the tritons from the (d,t) reaction on ^{12}C, due to its build up on the target during the experiment as well as on the ^{16}O and ^{27}Al nuclei, belonging to the material of target backing, do not interfere with the measured peaks, as these reactions are highly endothermic.

The measured angular distributions of deuterons and tritons from the reaction ^{7}Li$(d,t)^6$Li, as is seen in the figures given in the next chapter, have a well-defined diffraction structure, disappearing for large angles. The inelastic scattering with excitation of the 0.478 MeV ($1/2^-$) state gives the angular distribution with oscillations, as is expected, out of phase with the elastic cross section.

The statistical errors of the measured differential cross sections do not exceed 10%.

3. Analysis and discussion of results

3.1. Role of channel coupling and exchange mechanism

Calculations of the cross sections for the deuteron scattering and reaction ^{7}Li$(d,t)^6$Li were done in the framework of the coupled reaction channels (CRC) method using the FRESCO [14] program. Only the one step processes with neutron pick-up and exchange mechanism with the α-particle cluster transfer ^{7}Li$(d,\ ^6$Li$)t$, shown in Fig. 2, were taken into account. In our calculations, the system of nine nucleons presented in the entrance channel as ^{7}Li + d were replaced by three subsystems:

I. d+^{7}Li (g.s., $J^\pi = 3/2^-$; $E_x = 0.478$, $J^\pi = 1/2^-$),

II. t+^{6}Li (g.s., $J^\pi = 1^+$; $E_x = 2.186$, $J^\pi = 3^+$),

III. ^{6}Li (g.s., $J^\pi = 1^+$; $E_x = 2.186$, $J^\pi = 3^+$) + t.

The coupling scheme is shown in Fig. 3. All states of subsystems II and III are coupled with subsystem I by the reactions with neutrons and α-particles transfers. Couplings between ground and excited states of nuclei ^{7}Li and ^{6}Li were calculated using the rotational model with the form factor

$$V_\lambda(r) = \frac{\delta_\lambda}{\sqrt{4\pi}} \frac{dU(r)}{dr}$$

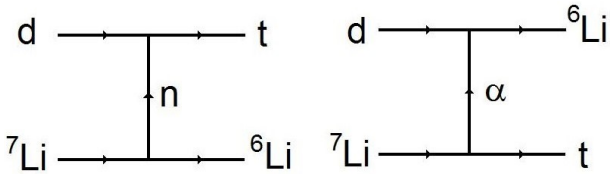

Fig. 2. Diagrams of the one-step neutron pick-up and α-particles exchange mechanisms.

for quadrupole transitions ($\lambda = 2$). Here, δ_λ is deformation length $\delta_\lambda = \beta_\lambda R$. The reorientation effects, determined by the matrix element $\langle E, J^\pi | V_2 | E, J^\pi \rangle$ were also included in the coupling scheme (Fig. 3). However, it should be noted that the collective model can be applied to such nuclei as ^{6}Li and ^{7}Li with one comment. In this case, strengthening of the quadrupole transitions is not connected with the usual quadrupole deformation, as for heavier nuclei. The ^{6}Li and ^{7}Li nuclei have a very pronounced cluster structure and very low binding energies of clusters with respect to the $^6\text{Li} \to \alpha + d$ and $^7\text{Li} \to \alpha + t$ decays. The deformation is rather related here to their dumbbell shape arising from separation of clusters.

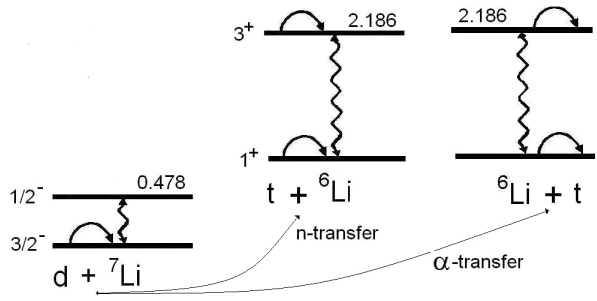

Fig. 3. The coupling scheme used in the CRC calculations for the $^7\text{Li}(d,t)^6\text{Li}$ reaction. The arcs show the spin reorientations of ^{7}Li and ^{6}Li nuclei in ground and excited states.

The prior representation of DWBA with a finite range interaction, incorporated in the FRESCO code was used in the calculations of neutron and α-particle transfer reactions. The wave functions of the bound states of $^7\text{Li} \to {}^6\text{Li} + n$ $(1P)$, $^7\text{Li} \to \alpha + t$ $(2P)$, $^6\text{Li} \to \alpha + d$ $(2S)$ for the ground and $1D$ for excited state and $t \to d + n\,(1S)$ were calculated in a standard way by fitting a depth of the real part of the Woods–Saxon potentials, giving the known binding energy ("well-depth"-procedure). Geometric parameters of the potentials (radii and diffuseness) were fixed (see Table I).

TABLE I

Geometric parameters of the Woods–Saxon potentials used in the calculation of the bound state wave functions.

System	R [fm]	a [fm]
$^6\mathrm{Li}+n$	2.31	0.65
$d+n$	1.85	0.65
$d+\alpha$	2.33	0.65
$t+\alpha$	2.48	0.65

Spectroscopic amplitudes for the $d + n$ (SA = 1.2247) and $\alpha + t$ (SA = 1.093) configurations were taken from the theoretical calculations in the framework of the translationary invariant shell model [15]. The remaining spectroscopic amplitudes were determined by fitting the calculated angular distributions to the experimental data.

The ground state ($3/2^-$) of the ^{7}Li nucleus was described as an interaction of the ^{6}Li (1^+) core with a neutron in the states $j = 1/2$ and $3/2$, according to the shell model. It is well known that the shape of the calculated angular distributions is determined by the transferred orbital angular momentum ($l = 1$) only and practically independent on j. Therefore, at absence of the experimental information about polarization, only summed value of the spectroscopic factors $S = S_{1/2} + S_{3/2}$ can be extracted in our analysis. Nevertheless, the calculations were performed with spectroscopic amplitudes for $j = 1/2$ and $j = 3/2$, using as starting their theoretical values [15]. Calculations were performed with the optical potentials listed in Table II.

TABLE II

Optical potentials used in the coupled reaction channels calculation of the scattering and $^7\mathrm{Li}(d,t)^6\mathrm{Li}$ reaction cross sections at the deuteron beam with the 25 MeV energy.

Set	System	V [MeV]	r_V [fm]	a_V [fm]	$W^*_{V/D}$ [MeV]	r_W [fm]	a_W [fm]	V_{SO} [MeV]	r_{SO} [fm]	a_{SO} [fm]	r_{C} [fm]	Ref.
1	$^7\mathrm{Li}+d$	81.14	1.17	0.91	11.09 D	1.325	0.75	6.76	1.07	0.66	1.3	[16]
	$^6\mathrm{Li}+t$	113.0	1.15	0.74	20.80 D	1.220	0.80	4.00	1.15	0.80	1.3	[17]
2	$^7\mathrm{Li}+d$	81.14	1.17	0.91	10.09 D	1.325	0.75	6.76	1.07	0.66	1.3	[16]
	$^6\mathrm{Li}+t$	120.0	1.15	0.65	30.00 V	1.460	0.85	4.00	1.15	0.80	1.3	[17]
3	$^7\mathrm{Li}+d$	90.00	1.15	0.81	9.60 D	1.340	0.87	6.00	1.15	0.81	1.3	[19]
	$^6\mathrm{Li}+t$	120.0	1.15	0.65	25.00 V	1.46	0.85	4.00	1.15	0.80	1.3	[18]
4	$^7\mathrm{Li}+d$	74.00	1.24	0.74	12.70 D	1.240	0.74	10.44	0.82	1.05	1.3	[20]
	$^6\mathrm{Li}+t$	171.0	1.11	0.69	17.00 V	1.39	0.59	1.72	1.36	1.18	1.3	[20]

* V — potential with volume absorption, D — potential with surface absorption.

Four sets of the optical potentials (OP) for the input $d + {}^7\mathrm{Li}$ and output $t + {}^6\mathrm{Li}$ channels obtained from analysis of the elastic scattering of deuterons and ${}^3\mathrm{He}$ on ${}^7\mathrm{Li}$ and ${}^6\mathrm{Li}$ nuclei respectively, at the incident particle energies in the range of 25–35 MeV [16–20] were used. Some of the potentials in Table II have been successfully tested before in the coupled reaction channels analysis of the reaction ${}^6\mathrm{Li}({}^3\mathrm{He}, d){}^7\mathrm{Be}$ at the energy 34 MeV [18]. It should be noted that the initial parameters of the potentials used in this calculation were obtained from the analysis of the elastic scattering only without consideration of the coupling with the inelastic channels, as well as with the reaction ${}^7\mathrm{Li}(d, t){}^6\mathrm{Li}$ and of the exchange mechanism of the α-particle transfer ${}^7\mathrm{Li}(d, {}^6\mathrm{Li})t$. Involvement in the consideration of additional processes within the coupled channel method usually requires modification of only the imaginary part of the potential needed for better agreement of the theoretical cross sections of the elastic scattering with experimental data at large angles. In this case, such change has little effect on the elastic scattering cross section in the forward hemisphere. To reduce ambiguity in search procedure, only the depths (W_V, W_D) of imaginary potentials were varied at fixed values of the geometric parameters (r_W, a_W) which were close to the values of global potentials found, for example, in the [14, 17]. The optimal values of W_V, W_D are selected based on the best description of the experimental cross sections the elastic scattering at angles $\theta > 120°$.

TABLE III

Deformation lenghts (δ_2) and spectroscopic factors S (in parentheses are given the total angular momentum of the transferred neutron (j)).

δ_2 [fm]			$S(j)$			
Set	${}^7\mathrm{Li}$	${}^6\mathrm{Li}$	${}^7\mathrm{Li} \to {}^6\mathrm{Li} + n$	${}^7\mathrm{Li} \to {}^6\mathrm{Li}^* + n$	${}^6\mathrm{Li} \to \alpha + d$	${}^6\mathrm{Li}^* \to \alpha + d$
1	3.0	3.0	0.72 0.32(1/2) + 0.40(3/2)	0.57(3/2)	1.13	0.67
2	2.5	3.0	0.60 0.27(1/2) + 0.33(3/2)	0.46(3/2)	1.12	0.52
3	3.5	3.0	0.60 0.27(1/2) + 0.33(3/2)	0.46(3/2)	1.12	0.74
4	4.0	3.0	0.58 0.26(1/2) + 0.32(3/2)	0.37(3/2)	1.35	0.44
Averaged over all sets			0.63 0.28(1/2) + 0.35(3/2)	0.47(3/2)	1.18	0.59
Theory [15]			0.97 0.43(1/2) + 0.54(3/2)	0.54(3/2)	1.13	1.12
Theory [21]			0.72 0.29(1/2) + 0.43(3/2)	0.55(3/2)		

The deformation lengths, δ_2, and spectroscopic factors (S) obtained from the analysis with different sets of the OP are shown in Table III. Despite an equally good description of elastic scattering for the all sets of optical potentials (Fig. 4), spectroscopic factors (Table III) still have some spreading which characterizes the influence of the potential choice on extracted spectroscopic information. Averaged values of the SF obtained in the present studies are in reasonable agreement with the theoretical values calculated in the framework of the shell model [15, 21].

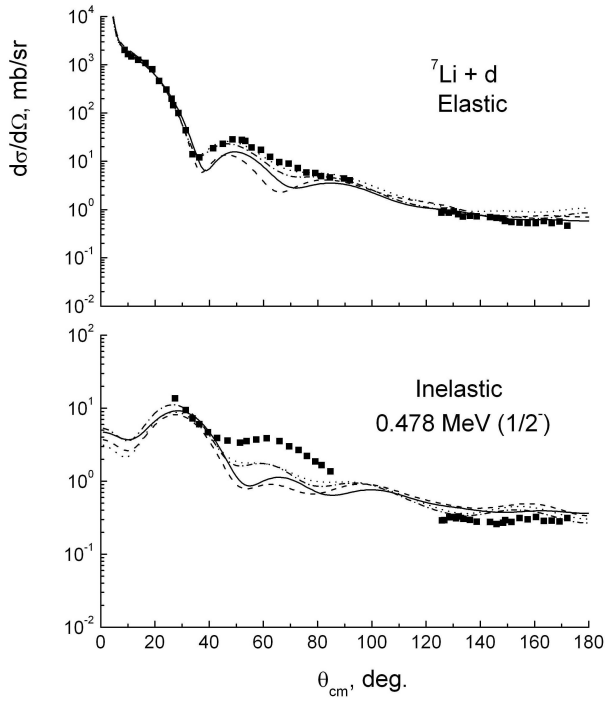

Fig. 4. Angular distributions of deuterons elastically and inelastically scattered on the ^{7}Li nuclei with excitation of $E_x = 0.478$ MeV $(1/2^-)$ state at the beam energy 25 MeV. Squares are experimental points. Curves — CRC calculations with all couplings shown in figure 3. The OP sets used in the calculations are in Table II: Set: 1 — dash-dotted, 2 — dotted, 3 — dashed and 4 — solid curves.

The comparison of calculated cross sections for elastic and inelastic scattering with excitation of the $E_x = 0.478$ MeV $(1/2^-)$ level of the ^{7}Li nucleus and the $^7\mathrm{Li}(d,t)^6\mathrm{Li}$ reaction with the transitions to the ground (1^+), and excited (3^+) states of ^{6}Li nucleus with experimental data is shown in Figs. 4 and 5 for different sets of the optical potentials from Table II. These curves were calculated taking into account all couplings shown in Fig. 3. One can

see that the calculations reproduce rather well the characteristic features of the experimental angular distributions at small (up to 40°–50°) and large angles, and only at the medium angles (50°–80°), the calculated cross sections are lower than the experimental ones.

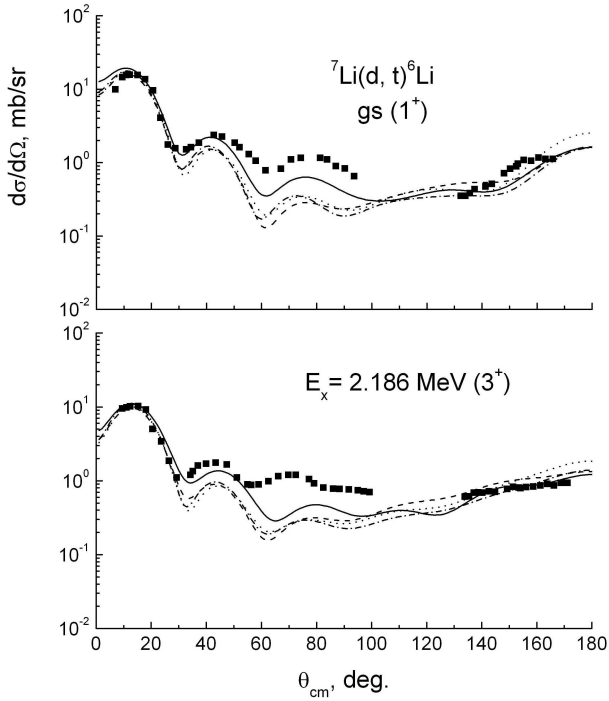

Fig. 5. Angular distributions of tritons from the reaction ^{7}Li$(d,t)^6$Li, corresponding to transitions to the ground (1^+) and the first excited state ($E_x = 2.186$ MeV (3^+)) states of ^{6}Li. Squares: experimental points. Curves: designations are the same as in Fig. 4.

The results of more detailed calculations for the set 4 (see Table II) are shown in Fig. 6. Dashed and dotted curves correspond to the direct neutron pick-up in the reaction ^{7}Li$(d,t)^6$Li and the exchange mechanism of the α-particles transfer in the ^{7}Li$(d,\ ^6$Li$)t$ reaction, respectively, calculated taking into account all couplings, shown in Fig. 3. Solid curves are their coherent sum. Generally, the analysis with using all sets of potentials shows that only contribution of the exchange mechanism allows to describe the behavior of the cross sections at large angles. Dash-dotted curves in Fig. 6 show the angular distributions of the tritons from direct neutron pickup mechanism in the reaction ^{7}Li$(d,t)^6$Li, calculated using the finite range DWBA (FRDWBA) with disabled links.

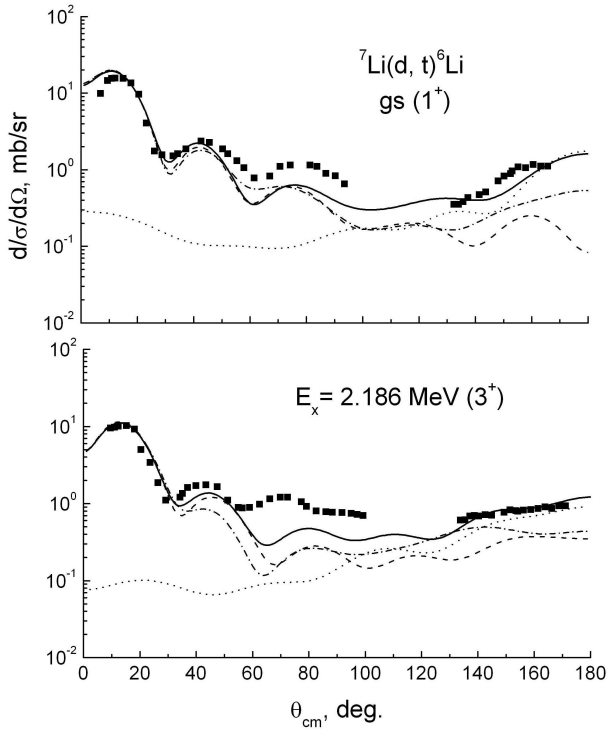

Fig. 6. Angular distributions of tritons from the reaction $^7\mathrm{Li}(d,t)^6\mathrm{Li}$, corresponding to transitions to the ground (1^+) and first excited ($E_x = 2.186$ MeV (3^+)) states of ^{6}Li nucleus. Squares — experimental points. Curves are calculations with OP of set 4 from Table II: Solid curves — all couplings were taken into account, dashed curves — all couplings in the $^7\mathrm{Li}(d,t)^6\mathrm{Li}$ process but without the contribution of α-particle transfer, dotted curves — transfer mechanism with α-particles exchange in the $^7\mathrm{Li}(d,\ ^6\mathrm{Li})t$ reaction. Dash-dotted curves — calculation of the reaction $^7\mathrm{Li}(d,t)^6\mathrm{Li}$ without coupling (FRDWBA).

Another important conclusion appeared from our analysis (it is well illustrated in Fig. 6): contribution of the coupled channels and exchange mechanism does not affect the behavior of the cross sections in the main maximum of the angular distributions (up to 40°–50° angles) and the pick-up mechanism dominates for angles up to 40°–50°. Contribution of other mechanisms, such as compound nuclear processes, as expected, is small and lies within the experimental errors. Indeed, these processes usually yield angular distributions that are symmetric about 90° in the center-of-mass system. Even if we assume that the entire cross sections at large angles are determined by the compound nucleus, its contribution at small angles will be no more than 10%. As a matter of fact, the cross section at angles of 140°–160° is fully reproduced by direct exchange mechanism with the trans-

fer of α-particles in the ^{7}Li$(d,\,^6$Li$)t$ reaction (Fig. 6) with reasonable values of the $^7\text{Li} \to \alpha + t$ and $^6\text{Li} \to \alpha + d$ spectroscopic amplitudes. Hence, the contribution of the compound nucleus will be considerably less, especially at small angles. These results as well as the peripheral character of the process allows us to use a modified distorted waves method to extract the values of the asymptotic normalization coefficients for the $^7\text{Li} \to {}^6\text{Li} + n$ system.

3.2. Analysis of the $^7Li(d,t)^6Li$ reaction using the modified distorted waves method

Below, we present the main features of the MDWBA in application to the $^7\text{Li}(d,t)^6\text{Li}$ reaction. According to [22, 23], for the pure peripheral neutron transfer (what is expected to be dominant within the main maximum of the tritons angular distribution), we can write the differential cross section in the form

$$\frac{d\sigma}{d\Omega} = \left(\frac{C_{0,1/2}}{b_{0,1/2}}\right)^2 C_{l,j}^2 R(E,\theta;b_{l,j})\,, \tag{1}$$

where

$$R\,(E,\theta;b_{l,j}) = \frac{\sigma\,(E,\theta;b_{l,j})}{b_{l,j}^2}\,. \tag{2}$$

Here, $C_{0,1/2} = C_t$ and $C_{l,j}$ are the ANCs, which determine the amplitudes of tails of the overlap functions for $t \to d + n$ and $^7\text{Li}_{\text{g.s.}} \to {}^6\text{Li} + n$ configurations; $b_{0,1/2} = b_t$ and $b_{l,j} = b$ are the asymptotical coefficients of the shell model wave functions for the bound $t \to d + n$ and $^7\text{Li}_{\text{g.s.}} \to {}^6\text{Li} + n$ states, respectively. In MDWBA formalism is assumed that the asymptotic behavior of the overlap integral of the radial wave functions and model wave functions is the same and corresponds to the Hankel function of the first order [8]. $\sigma(E,\,\theta;\,b_{l,j})$ is the single particle cross section of neutron transferring, calculated by code DWUCK5. The values E and θ are the relative kinetic energy of the interacting nuclei in the entrance channel and the emission angle of the triton in the CM-system.

The values of the total angular momentum of the transferred neutron are $j = 1/2$ or $3/2$ for ground and $j = 3/2$ for $E_x = 2.186$ MeV excited states of the ^{6}Li final nucleus at the transferred orbital momentum $l = 1$ for the considered reaction. As is shown in [24], the square of the ANC (C^2) is explicitly related to the square of the modulus of nuclear vertex constants ($|G|^2$) and spectroscopic factor (S) for any vertex $B \to A+d$ by the following expression (indexes are omitted)

$$C^2 = \left[(\mu c/\hbar)^2/\pi\right]|G|^2 = Sb^2\,, \tag{3}$$

where μ is the reduced mass of the particles A and d.

So, seemingly, one could obtain the ANC directly through the spectroscopic factor, extracted from the analysis of the experimental differential cross sections using the FRESCO program and the value $b_{l,j}$ determined from the asymptotic behavior of solution of the Schrödinger equation for the bound state of ^{6}Li + n with the Woods–Saxon binding potential. However, in this case, one must be assured that the transfer of the neutron is a peripheral one-step process. Only at this case, the spread of extracted ANC values conditioned by ambiguities of the geometric parameters of the bound state potential will be small enough (unlike S values). The MDWBA provides the possibility to ensure that the reaction proceeds through the tail of the appropriate overlap function and to evaluate the model uncertainties of the obtained ANC value. In MDWBA formalism, function $R(E,\theta;b_{l,j}) = R(b)$ should not substantially depend on the $b_{l,j}$ (see, for example, [25]) and, consequently, on varying the potential geometric parameters of the bound state, if the transfer occurs at the periphery of interacting nuclei. It should be stressed that both b_j and $\sigma(E,\theta;b_{l,j})$, and hence, SF depend strongly on the geometric parameters.

To confirm the peripheral character of the neutron transferring in the area of main peak of tritons angular distribution from the ^{7}Li$(d,t)^6$Li reaction, the behavior of the function $R(b)$ (2) was analyzed. The area of values of the $R(b)$ function is shown in Fig. 7 at values r_0 and a within physically reasonable ranges of these parameters $1.0 \div 1.5$ fm and $0.45 \div 0.85$ fm, respectively. The calculations were carried out with the set 4 of OP from Table II for the triton emission angle corresponding to the main maximum

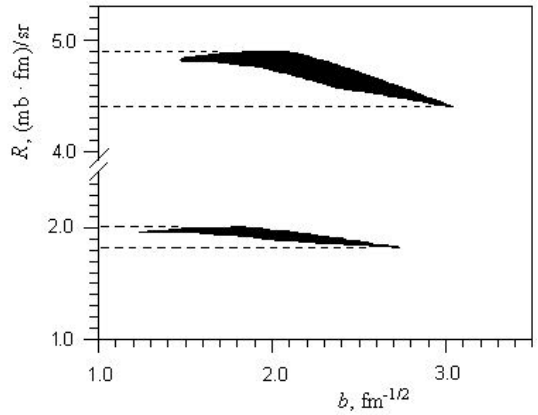

Fig. 7. Range of $R(b)$ values for the ^{7}Li$(d,t)^6$Li reaction for varying values of geometrical parameters r_0, a, within the intervals 1.0 fm–1.5 fm and 0.45 fm–0.85 fm, respectively. Excitations of ^{6}Li: $E_x = 0.0$ MeV (1^+) — top, $E_x = 2.186$ MeV (3^+) — bottom.

of the angular distribution, $\theta_{\rm CM} = 12^\circ$. One can see that the function $R(b)$ weakly depends (within $\pm 5\%$) on the geometrical parameters in the ranges shown above for both ground and excited states of ^{6}Li. A similar result was obtained with other sets of OP from Table II, indicating that the neutron pick-up is peripheral at least for tritons emitted to small angles. On the other hand, as it follows from the analysis performed in Subsection 3.1, the neutron pick-up process dominates in this angular region. Thus, using equations (1) and (2), it is correct to evaluate the square ANC value for ^{7}Li $\rightarrow$ ^{6}Li + n by means of SF values and the corresponding values b_{lj} from Table IV. But the more correct way is using relation (3) with the values of SF, obtained in Subsection 3.1 accounting the contribution of other possible mechanisms.

It should be emphasized, as mentioned above, that the extracted value of spectroscopic factor S_{lj} for (^{6}Li + n) configuration strongly depends on the geometrical parameters of the bound state potential. As is shown in Fig. 8, the value of SF is changed to five times along their variation in the mentioned above range, whereas the square of the ANC in this case varies in a range of 5% only. At the same time, strong variations of the value S_{lj} are compensated by opposite phase variations of the value of single-particle asymptotic coefficient b_{lj}.

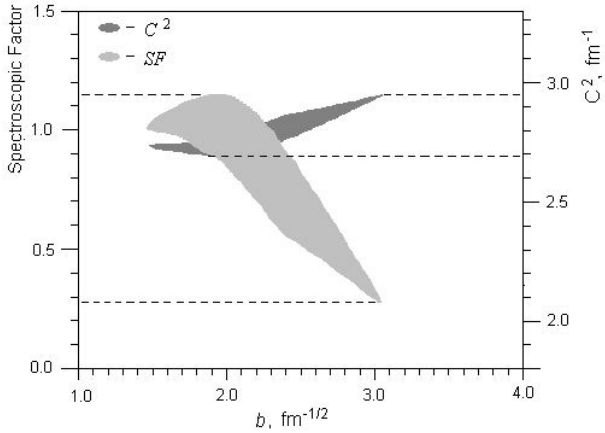

Fig. 8. Ranges of SF and square values of ANC, corresponding to variation of r_0, a parameters (and, hence, value of b), derived from MDWBA analysis of the ^{7}Li$(d,t)^6$Li$_{\rm g.s.}$ reaction.

The values of the ANC squares, calculated using formula (3) for the ground state of ^{7}Li with ^{6}Li core at the ground and excited ($E_x = 2.186$ MeV) states are shown in Table IV, column 5. In column 4, the corresponding calculated values of the asymptotic coefficients b_{lj} are presented. The squared

moduli of the vertex constants ($|G|^2$) for $^7\mathrm{Li} \to {}^6\mathrm{Li}_{\mathrm{g.s.}} + n$ and $^7\mathrm{Li} \to {}^6\mathrm{Li}_{2.186} + n$ vertices (see the polar diagram in Fig. 2, left) are shown in the sixth column. They were calculated using formula (3) with the obtained values S_{lj} and b_{lj}. The ($|G|^2$) values are in good agreement with the results of [8] for the deuteron energy 18 MeV (($|G|^2$) $= 0.60 \pm 0.10$ fm and 0.80 ± 0.09 fm for the vertices $^7\mathrm{Li} \to {}^6\mathrm{Li}_{\mathrm{g.s.}} + n$ and $^7\mathrm{Li} \to {}^6\mathrm{Li}_{2.186} + n$, respectively). This evidence indicates a lack of the energy dependence of the "experimental" ($|G|^2$) at least in the energy range of 18–25 MeV, which was mentioned in the introduction. Underestimation of the value ($|G|^2$) $= 0.3$ fm obtained in [8] from the analysis of the data [10] at $E_d = 28$ MeV, is apparently due to the fact that the experimental data include only the second and third diffraction maxima ($\theta > 40^\circ$) where the contribution of the exchange mechanism, as shown in Section 3.1, is not small.

TABLE IV

Averaged over the OP sets the spectroscopic factors S_{lj}, squares of ANC (C^2_{lj}) and squares of nuclear vertex constants ($|G|^2$) for corresponding systems.

System	l, j	S_{lj}	b_{lj} [fm]	C^2_{lj} [fm]	$\lvert G\rvert^2$ [fm]
$^7\mathrm{Li} \to {}^6\mathrm{Li}_{\mathrm{g.s.}} + n$	$1, 1/2$	0.28 ± 0.02	2.087	1.22 ± 0.17	
	$1, 3/2$	0.35 ± 0.03	2.176	1.66 ± 0.23	
	$1, 1/2 + 3/2$	0.63 ± 0.05	2.133	2.88 ± 0.40	0.55 ± 0.08
$^7\mathrm{Li} \to {}^6\mathrm{Li}_{2.186} + n$	$1, 3/2$	0.47 ± 0.06	2.841	3.79 ± 0.59	0.73 ± 0.11

Errors of spectroscopic factors, listed in Table IV, include the standard deviations of averaging over sets of OP. Absolute errors for the ANC squares include, in statistically independent way, the experimental errors in the differential cross sections of the main maximum angular region, the model uncertainties due to the ambiguity of the parameters of the neutron binding potential (see Fig. 7) and spread of values conditioned by ambiguity of the OP parameters in the entrance and exit channels.

The values of neutron spectroscopic factors for a number of nuclei were extracted in [26] from analysis of the angular distributions of the (p, d) and (d, p) reactions. In particular, for $^7\mathrm{Li}_{\mathrm{g.s.}} \to {}^6\mathrm{Li} + n$, the value $S = S_{1,1/2+3/2} = 1.85 \pm 0.37$ was obtained from the $^7\mathrm{Li}(p, d)^6\mathrm{Li}$ reaction. This is in contradiction not only with theoretical predictions (see Table III), but also with results of analysis of the inverse reaction (d, p), performed by the authors of the same paper [26] ($S = 1.12 \pm 0.32$) and with our result ($S = 0.63 \pm 0.05$). The discrepancy can be explained by the fact that the reaction $^7\mathrm{Li}(p, d)^6\mathrm{Li}$ is not peripheral (as it has been shown in [8]), since the value R is strongly dependent on the value of b (see formula (2)). Consequently, it cannot be used to obtain the reliable spectroscopic information

within the distorted-wave method. Then, the peripheral character of the ^{7}Li$(d,t)^6$Li reaction, as it was shown by our analysis and by the data of [8], is not in doubt.

It is also interesting to compare the values of ANC for the neutron and proton binding at ground states of the mirror nuclei ^{7}Li and ^{7}Be. There is an active discussion in recent years concerning the accuracy of a strong correlation between them (see [27] and references therein). Indeed, if the spectroscopic factors of these states are equal, relation (3) implies: $C_p^2/C_n^2 = b_p^2/b_n^2$. This means that the parameters of the nuclear potentials of bound states of the proton and neutron are equal. Equality of the nuclear parts of the binding potentials at the observed separation energies of nucleons ("well-depth"-procedure) is achieved for the Coulomb radius parameter values $r_C = 1.575$ fm for $j_p = 1/2$ and $r_C = 1.515$ fm for $j_p = 3/2$. Therewith, the value b_p^2 and so, the ratio b_p^2/b_n^2 for the mirror states practically does not depend on the parameter r_C, as was shown in [28]. Moreover, our estimations show that the values S, C_p^2, b_p vary only within 0.2% when the r_C changes from 1.3 fm to 1.52 fm. The empirical square value of the ANC, $C^2_{^7\mathrm{Be}\to^6\mathrm{Li}+p}$, obtained from analysis of the reaction ^{6}Li(^{3}He, d)^{7}Be in MDWBA formalism is 3.13 ± 0.27 fm^{-1} [18]. The single-particle asymptotic coefficients b_{lj} for $^7\mathrm{Be}_{\mathrm{g.s.}} \to {}^6\mathrm{Li} + p$ configuration are 2.145 fm$^{-1/2}$ ($j_p = 1/2$) and 2.234 fm$^{-1/2}$ ($j_p = 3/2$), and the average value $b_p = 2.190$ fm$^{-1/2}$ for the mentioned above nuclear — equivalent potential of a bound state. At the same time, taking into account the values b_{1j} and C_{lj}^2 from Table IV for the neutron bound state, the b_p^2/b_n^2 and C_p^2/C_n^2 ratios are 1.05 ± 0.10 and 1.09 ± 0.10, *i.e.* well satisfy the $C_p^2/C_n^2 = b_p^2/b_n^2$ relation within the error limits.

4. Conclusions

The differential cross sections for elastic and inelastic scattering with excitation of the 0.478 MeV ($1/2^-$) of ^{7}Li nuclei in the angular range of 8°–169° (LAB) as well as the cross sections of the reaction ^{7}Li$(d,t)^6$Li with transitions to the ground (1^+) and excited ($E_x = 2.186$ MeV, 3^+) state of the ^{6}Li have been measured at the deuteron beam with the 25 MeV energy.

The experimental angular distributions were analyzed in the framework of the coupled reaction channels (CRC) method, with taking into account the exchange mechanism ^{7}Li$(d,\,^6\mathrm{Li})t$ with α-particle transfer. It was shown, that the channel coupling affects the triton emission cross sections only at angles greater than 40°. In the main maximum of the angular distributions for the ^{7}Li(d,t) ^{6}Li reaction, the CRC and the DWBA give an equivalent description of the experimental data. It was established that the mechanism of the one-step neutron pick-up dominates at angles up to 40° and the reaction occurs on the surface of a nucleus.

The values of spectroscopic factors for $^7\mathrm{Li} \to {}^6\mathrm{Li} + n$ and $^7\mathrm{Li} \to {}^6\mathrm{Li}^* + n$ systems were obtained by comparison of the calculated angular distributions with experimental data. The results are close to the theoretical predictions. The domination of the pick-up mechanism at forward angles of triton emission and peripheral character of the $^7\mathrm{Li}(d,t)^6\mathrm{Li}$ reaction gives a possibility to obtain the reliable values of the ANC for ground state of ^{7}Li nucleus in $^7\mathrm{Li} \to {}^6\mathrm{Li}_{\mathrm{g.s.}} + n$ ($C^2_{lj} = 2.88 \pm 0.40$ fm^{-1}) and $^7\mathrm{Li} \to {}^6\mathrm{Li}_{2.186} + n$ ($C^2_{lj} = 3.79 \pm 0.59$ fm^{-1}) configurations. It was shown that the square of the ANC for $^7\mathrm{Li} \to {}^6\mathrm{Li}_{\mathrm{g.s.}} + n$ configuration satisfy theoretically predicted ratio $C^2_p/C^2_n = b^2_p/b^2_n$ for mirror nuclei ^{7}Li and ^{7}Be and is consistent with the value obtained in [18].

This work was supported in part by a grant of MES RK Project "Experimental and theoretical investigation of elastic and quasi-elastic processes of interaction of ^{3}He and d ions with nuclei of p- and sd-shell".

REFERENCES

[1] S.N. Abramovich, B.Ya. Guzhovsky, B.A. Zherebtsov, A.G. Zvenigorodsky, *Yaderno-fisicheskie Konstanty Termoyadernogo Sinteza*, in Russian, Moscow 1989.

[2] K.M. Nollett, M. Lemoine, D.N. Schramm, *Phys. Rev.* **C56**, 1144 (1997).

[3] E. Rollinde, E. Vangioni-Flam, K.A. Olive, *Astrophys. J.* **627**, 666 (2005).

[4] A.R. Zander, K.W. Kemper, N.R. Fletcher, *Nucl. Phys.* **A173**, 273 (1971).

[5] M.F. Werby, S. Edwards, *Phys. Rev.* **C8**, 978 (1973).

[6] S.H. Levine, R.S. Bender, J.N. McCruer, *Phys. Rev.* **97**, 1249 (1955).

[7] E.W. Hamburger, J.R. Cameron, *Phys. Rev.* **117**, 781 (1960).

[8] I.R. Gulamov, A.M. Mukhamedzhanov, G.K. Nie, *Phys. Atom. Nucl.* **58**, 1689 (1995); *Yad. Fiz.* **58**, 1789 (1995).

[9] A.A. Ogloblin, *Nucl. Phys.* **47**, 408 (1963).

[10] R.J. Slobodrian, *Phys. Rev.* **126**, 1059 (1962).

[11] D.R. Tilley *et al.*, *Nucl. Phys.* **A708**, 3 (2002).

[12] M. Bouten, M.C. Bouten, P. van Leuven, *Nucl. Phys.* **A100**, 105 (1967).

[13] S.V. Artemov *et al.*, *Izv. MON RK, NAN RK, Ser. Fiz. Mat.* **6**, 61 (2006).

[14] I.J. Thompson, *Comput. Phys. Rep.* **7**, 167 (1988).

[15] O.F. Nemets *et al.*, *Nucleons Associations in Atomic Nuclei and Multi-nucleon Transfer Reactions*, in Russian, Naukova Dumka, 1988.

[16] N. Burtebayev *et al.*, *AIP Conf. Proc.* **203**, (2008).

[17] D.Y. Pang *et al.*, *Phys. Rev.* **C79**, 024615 (2009).

[18] N. Burtebayev *et al.*, *Nucl. Phys.* **A909**, 20 (2013).
[19] A.K. Basak *et al.*, *Nucl. Phys.* **A368**, 74 (1981).
[20] C.M. Perey, F.G. Perey, *At. Data Nucl. Data Tables* **17**, 1 (1976).
[21] S. Cohen, D. Kurath, *Nucl. Phys.* **A101**, 1 (1967).
[22] A.M. Mukhamedzhanov *et al.*, *Phys. Rev.* **C56**, 1302 (1997).
[23] S.V. Artemov *et al.*, *Phys. Atom. Nucl.* **71**, 998 (2008); *Yad. Fiz.* **71**, 1025 (2008).
[24] L.D. Blokhintsev, I. Borbey, E.I. Dolinskii, *Fiz. Elem. Chastits i At. Yadra.* **8**, 1189 (1977) (in Russian); *Sov. J. Part. Nucl.* **8**, 485 (1977).
[25] S.V. Artemov, E.A. Zaparov, G.K. Nie, *Izv. RAN, Ser. Fiz.* **67**, 1577 (2003) (in Russian); *Bull. Rus. Acad. Sci. Phys.* **67**, 1741 (2003).
[26] M.B. Tsang, J. Lee, W.G. Lynch, *Phys. Rev. Lett.* **95**, 222501 (2005).
[27] L.J. Titus, P. Capel, F.M. Nunes, *Phys. Rev.* **C84**, 035805 (2011).
[28] G.K. Nie, S.V. Artemov, *Bull. Rus. Acad. of Sci. Phys.* **71**, 1762 (2007).